

Dynamics of Delaminated Composite Plates with Piezoelectric Actuators

Aditi Chattopadhyay*, Haozhong Gu,[†] and Dan Dragomir-Daescu[‡]
Arizona State University, Tempe, Arizona 85287-6106

A refined higher-order-theory-based finite element model is developed for modeling the dynamic response of delaminated smart composite plates. The theory assures an accurate description of displacement field and the satisfaction of stress-free boundary conditions at all free surfaces including delamination interfaces. A nonlinear induced strain model is used. Vibration control is obtained through piezoelectric layers bonded on the composite plate. The theory is implemented using a finite element technique, which allows the incorporation of practical geometries and boundary conditions, various sizes, and locations of delaminations, as well as discrete sensors and actuators. The resulting model is shown to agree well with published experimental data. Significant changes in dynamic properties are observed due to the presence of delamination.

Nomenclature

a	= plate length
b	= plate width
c^r	= midplane positions for different regions
D	= electric displacement matrix
d	= strain coefficient matrix
d^r	= local region thickness
E	= electric field intensity
F	= external force vector
F_p	= piezoelectric force vector
h	= plate thickness
h_1	= delamination position
i_k	= current
K	= global stiffness matrix
K^e	= element kinetic energy
M	= global mass matrix
P	= dielectric permittivity matrix
Q, Q_k	= stiffness matrices
q_k	= electric charge
S	= interface between undelaminated and delaminated regions
T^k	= transformation matrix
U^e	= element strain energy
U^r, V^r, W^r	= displacement field functions
u^r, v^r, w^r	= midplane displacements
u_s^r, u_s^k	= nodal generalized displacement vector in undelaminated and delaminated regions
W^e	= element work done
β	= delamination length
ε	= strain vector
Π	= total potential energy
σ	= stress vector
ψ_x^r, ψ_y^r	= supplementary rotation functions
Ω^a, Ω^b	= undelaminated, above, and below delamination regions, respectively

I. Introduction

SMART composite materials offer the potential for designing structures that are lightweight and possess adaptive control

capabilities for shape correction and vibration control. In designing with composites, one must take into consideration imperfections, such as delamination, that are often preexisting or are generated by external impact forces during the service life. The existence of delamination can significantly alter the dynamic response of smart composite structures.¹ Several mathematical models have been reported in the literature for the analysis of beams and plates with piezoelectric sensing/actuation. The classical-theory-based approach² was first introduced to investigate such problem with thin beams. This was followed by the first-order Mindlin type analyses³ and the expensive layerwise theories.⁴ A hybrid theory has also been reported.⁵ It is well known that refined higher-order theories are capable of capturing the transverse shear deformation through the thickness quite accurately.⁶ These theories are applicable for laminates of thicker construction and have been shown to be useful in modeling smart composite laminates.¹ Finite element-based solution procedures^{3,7} are practical because real geometries and boundary conditions can be investigated.

A significant amount of research has also been performed in modeling delamination in composites. Although three-dimensional approaches⁸ are more accurate than two-dimensional theories,⁹ their implementation can be very expensive for practical applications. The layerwise approach¹⁰ is an alternative because it is capable of modeling displacement discontinuities. However, the computational effort increases with the number of plies. A refined higher-order theory, developed by Chattopadhyay and Gu,⁶ was shown to be both accurate and efficient for modeling delamination in composite plates and shells of moderately thick construction. This theory has also been shown to agree well with both elasticity solutions¹¹ and experimental results.¹²

Preliminary research¹³ has also been conducted on the use of smart materials for detecting preexisting delamination. However, the mathematical models used in these works are simply classical-theory-based approaches, which exclude the transverse shear effects. The importance of transverse shear deformation in composite laminates has been identified by many researchers. Deviations in structural response of as much as 50% have been reported in thick constructions.^{6,10} Recently, Seeley and Chattopadhyay¹⁴ introduced the higher-order theory in the analysis of adaptive composite plates in the presence of debonding between the laminate and the actuator. It was shown that the presence of debonding significantly changes the dynamic response.

The objective of the current research is to develop a mathematical model for the dynamic analysis of delaminated smart composite laminates using a refined higher-order theory. The theory is implemented using the finite element approach. The model also carefully accounts for the distributed nature of discrete delaminations, actuators, and sensors in the primary structure. Because the relationships between the induced strain due to actuation and the applied electric field are nonlinear in nature,¹⁵ a nonlinear analytical induced

Received March 30, 1998; revision received Sept. 16, 1998; accepted for publication Sept. 27, 1998. Copyright © 1998 by the authors. Published by the American Institute of Aeronautics and Astronautics, Inc., with permission.

*Professor, Department of Mechanical and Aerospace Engineering, Associate Fellow AIAA.

[†]Postdoctoral Fellow, Department of Mechanical and Aerospace Engineering, Member AIAA.

[‡]Graduate Research Associate, Department of Mechanical and Aerospace Engineering, Member AIAA.

strain formulation is used in the current research.¹⁶ A control algorithm is implemented for vibration reduction of delaminated smart composite plates.

II. Mathematical Formulation

A refined higher-order theory is extended to model dynamics of smart composite laminates in the presence of delaminations. The details of the formulation are presented in this section.

A. Higher-Order Displacement Field

A general higher-order displacement field is extended to model composite plates with induced strain actuation due to piezoelectric materials (Fig. 1). The in-plane displacements are assumed to be effectively expressed by a cubic function through the thickness z , and the transverse displacement is assumed to be independent of z . To model delamination in such structures, it is necessary to partition the laminate into several different regions as shown in Fig. 2. These regions include the undelaminated region Ω^u , the region above the delamination Ω^a , and the region below the delamination Ω^b . The interface between the undelaminated region and the delaminated region, indicated by the dashed line in Fig. 2, is denoted S . The general form of the higher-order displacement field is independently applied to each of these regions to describe displacements that account for slipping and separation due to the delamination. This general form does not satisfy the stress-free boundary conditions. Applying the traction-free boundary condition at the top and bottom surfaces of the plate ($z = \pm h/2$) as well as on the delamination interface ($z = h_1$) in the delaminated region, a refined displacement field can be obtained:

$$\begin{aligned} U^r(x, y, z) &= u^r(x, y) + (z - c^r) \left[\psi_x^r(x, y) - \frac{\partial w^r(x, y)}{\partial x} \right] \\ &\quad - \frac{4(z - c^r)^3}{3(d^r)^2} \psi_x^r(x, y) \\ V^r(x, y, z) &= v^r(x, y) + (z - c^r) \left[\psi_y^r(x, y) - \frac{\partial w^r(x, y)}{\partial y} \right] \\ &\quad - \frac{4(z - c^r)^3}{3(d^r)^2} \psi_y^r(x, y) \quad r = u, a, b \\ W^r(x, y, z) &= w^r(x, y) \end{aligned} \quad (1)$$

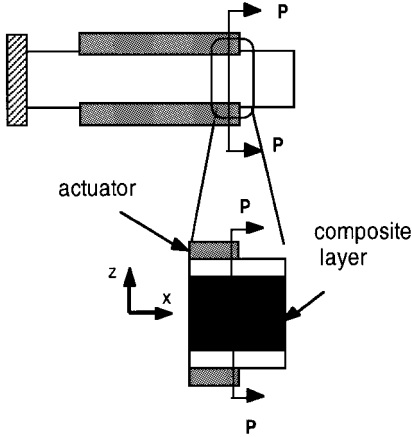


Fig. 1 Cantilever composite laminate with piezoelectric actuators.

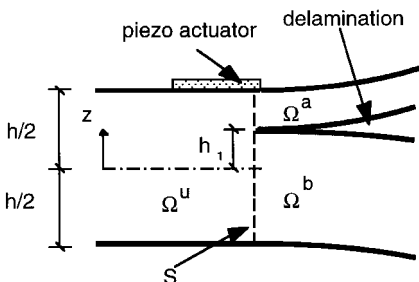


Fig. 2 Laminate cross section.

where U , V , and W are the in-plane and out-of-plane displacements at a point (x, y, z) ; ψ_x and ψ_y represent the midplane rotations. The superscript r corresponds to either the undelaminated region u or the regions above and below the delamination a and b , respectively.

B. Constitutive Relations

For an anisotropic elastic body, the constitutive relations among the stress, strain, charge, and electric field can be derived from the electric enthalpy density function as follows:

$$H(\varepsilon_{ij}, E_i) = \frac{1}{2} c_{ijkl} \varepsilon_{ij} \varepsilon_{kl} - e_{ijk} E_i \varepsilon_{jk} - \frac{1}{2} k_{ij} E_i E_j \quad (2)$$

where ε_{ij} and E_i are components of the strain tensor and electric field vector, respectively, and c_{ijkl} , e_{ijk} , and k_{ij} are the elastic, piezoelectric, and dielectric permittivity constants, respectively. The stress and charge are then determined as

$$D_i = -\frac{\partial H}{\partial E_i}, \quad \sigma_{ij} = \frac{\partial H}{\partial \varepsilon_{ij}} \quad (3)$$

For an orthotropic composite plate with piezoelectric layers, the constitutive relationships can be written as follows^{1,14}:

$$\hat{\sigma}_k = \mathbf{Q}_k (\hat{\varepsilon}_k - \mathbf{d}_k \mathbf{E}_k), \quad \mathbf{D}_k = \mathbf{d}_k^T \mathbf{Q}_k \hat{\varepsilon}_k - \mathbf{P}_k \mathbf{E}_k \quad (4)$$

where

$$\begin{aligned} \hat{\sigma}_k &= [\sigma_x \quad \sigma_y \quad \tau_{yz} \quad \tau_{xz} \quad \tau_{xy}]_k^T \\ \hat{\varepsilon}_k &= [\varepsilon_x \quad \varepsilon_y \quad \gamma_{yz} \quad \gamma_{xz} \quad \gamma_{xy}]_k^T \end{aligned} \quad (5)$$

$$\mathbf{d}_k = \begin{bmatrix} 0 & 0 & d_{31} \\ 0 & 0 & d_{32} \\ 0 & d_{24} & 0 \\ d_{15} & 0 & 0 \\ 0 & 0 & 0 \end{bmatrix}_k$$

$$\mathbf{Q}_k = \begin{bmatrix} \bar{Q}_{11} & \bar{Q}_{12} & 0 & 0 & \bar{Q}_{16} \\ \bar{Q}_{12} & \bar{Q}_{22} & 0 & 0 & \bar{Q}_{26} \\ 0 & 0 & \bar{Q}_{44} & \bar{Q}_{45} & 0 \\ 0 & 0 & \bar{Q}_{45} & \bar{Q}_{55} & 0 \\ \bar{Q}_{16} & \bar{Q}_{26} & 0 & 0 & \bar{Q}_{66} \end{bmatrix}$$

In the preceding equations, $\hat{\sigma}$ and $\hat{\varepsilon}$ denote the stress and the mechanical strain in the material coordinates, respectively. According to Crawley and Lazarus,¹⁵ the coefficients d_{ij} depend on the actual strain in the actuator as well. However, due to the weak nonlinearity, they can be rewritten using first-order Taylor series expansion as follows:

$$d_{ij} = d_{ij}(\varepsilon_j) = d_{ij}^0 + d_{ij}^1 \varepsilon_j + \frac{1}{2} d_{ij}^2 \varepsilon_j^2 + \dots \cong d_{ij}^0 + d_{ij}^1 \varepsilon_j \quad (6)$$

The coefficients d_{ij}^0 and d_{ij}^1 can be identified using functional relationships of the strain vs the electric field obtained from the experimental data of an unconstrained piezoelectric actuator.

C. Continuity Conditions

Additional continuity conditions must be imposed to ensure the continuity of displacements at the interface of the undelaminated and the delaminated regions S as shown in Fig. 2. The continuity conditions at the interface of the undelaminated and the delaminated regions are imposed as follows:

$$\begin{aligned} U^u &= U^a, & V^u &= V^a, & W^u &= W^a \\ U^u &= U^b, & V^u &= V^b, & W^u &= W^b \end{aligned} \quad x \in S \quad (7)$$

The relations of displacement fields defined in different regions at region interface S can now be derived in the following matrix form:

$$\mathbf{u}_s^k = \mathbf{T}^k \mathbf{u}_s^u, \quad k = a, b \quad (8)$$

D. Control Equations

Because piezoelectric sensors can accurately detect strain rate when they are connected with a current amplifier and proportional feedback is the simplest to apply for structural vibration control, a piezoelectric sensor model is developed here for monitoring the proportional variables that are necessary for control feedback. When the k th piezoelectric sensor layer is deformed, it accumulates an electric charge on its surface electrode, which is given by

$$\mathbf{q}_k(t) = \int_A \int_z \mathbf{D}_k dz dA = \int_A \int_z \mathbf{Q} d\hat{\varepsilon}_k dz dA \quad (9)$$

The current developed from the electric charge is obtained by differentiating the charge equation [Eq. (9)] with respect to time:

$$\dot{\mathbf{q}}_k(t) = \dot{\mathbf{q}}_k(t) = \int_A \int_z \mathbf{Q} [d(\hat{\varepsilon}) \dot{\hat{\varepsilon}} + \dot{d}(\hat{\varepsilon}) \hat{\varepsilon}] dz dA \quad (10)$$

In designing a control law using the Lyapunov direct method, the structural stability in the Lyapunov sense is guaranteed if the feedback actuator voltage is selected as

$$\mathbf{E}_k(t) = G \dot{\mathbf{q}}_k(t) = G \int_A \int_z \mathbf{Q} [d(\hat{\varepsilon}) \dot{\hat{\varepsilon}} + \dot{d}(\hat{\varepsilon}) \hat{\varepsilon}] dz dA \quad (11)$$

with gain $G > 0$. The collocated sensor-actuator was used in this research. It is assumed that the energy stored in the electric field in the sensor is small enough compared with the actuator, and its effect can be neglected.

III. Finite Element Implementation

The finite element method is used to implement the refined higher-order theory because it allows for the analysis of practical geometries and boundary conditions. The finite element equations are derived using the discretized form of Hamilton's principle, which is stated as follows:

$$\delta \Pi = \int_{t_1}^{t_2} \sum_{e=1}^{N_e} [\delta K^e - \delta U^e + \delta W^e] dt = 0 \quad (12)$$

where t_1 and t_2 are the initial and the final times, respectively, and δK^e , δU^e , and δW^e represent the elemental variations in the kinetic energy, the strain energy, and the work done, respectively. The global finite element equations of motion are then expressed as follows:

$$\mathbf{M} \ddot{\mathbf{u}} + \mathbf{K} \mathbf{u} = \mathbf{F} + \mathbf{F}_p \quad (13)$$

A 16-term polynomial shape function is used for interpolating the out-of-plane displacements w , whereas bilinear shape functions are used for the other unknown functions (u , v , ψ_x , and ψ_y).

IV. Results and Discussions

Numerical results are presented first to compare the higher-order theory with published experimental results to validate its accuracy. Next, dynamic response and vibration control using piezoelectric actuation are presented for a cantilever composite plate with varying delamination lengths. The results are presented for [0 deg/90 deg], graphite/epoxy laminates with surface bonded piezoelectric actuator pairs. The material properties used for the smart composite plate are listed in Table 1, where E is Young's modulus and ν is Poisson's ratio. Plates with length $a = 0.127$ m, thickness $h = 0.001016$ m, and width $b = 0.0127$ m are considered. The piezo-

Table 1 Material properties

Property	Graphite/epoxy	PZT
E_1 , GPA	134.4	63
E_2 , GPA	10.3	63
ν_{12}	0.33	0.33
G_{12} , G_{13} , GPA	5	24.2
G_{23} , GPA	2	24.2
ρ , $\times 10^3$ kg/m ³	1.477	7.6
d_0 , $\times 10^{-12}$ m/V	—	24.7
d_1 , $\times 10^{-7}$ m/V	—	8.38

Table 2 First natural frequency for delamination along the midplane

Delamination length, mm	Experiment (average), Hz	Current higher-order theory, Hz
0	79.833	82.119
25.4	78.168	80.056
50.8	75.375	75.620
76.2	66.958	67.142
91.6	57.542	57.813

electric actuator-sensor pairs have dimensions of $L_p = 0.0127$ m, $h_p = 0.000254$ m, and $b_p = 0.0127$ m, located at different positions (see Fig. 1).

The results from the current approach are compared with experimental data obtained by Shen and Grady¹⁷ as shown in Table 2. Delamination lies on the midplane of the plate and starts from the clamped end. The natural frequencies obtained from the higher-order-theory-based finite element approach show good correlation with experimental data, especially in the delaminated case. This indicates that the higher-order-theory-based model provides an effective tool for modeling delamination.

The effect of closed-loop control due to piezoelectric actuation is investigated. The plate is released from an initially bent position, which is produced by a piezoelectric actuation due to 127 V. Three collocated sensor-actuator pairs are located at the top and bottom surfaces of the plate (Fig. 1). The three pairs of sensor-actuators are evenly located along the plate length, and the control gain for this example is selected as 1000. The internal structural damping is assumed to be 0.5% of critical damping for each normal coordinate. Figures 3a and 3b present the dynamic responses of undelaminated smart composite plates with and without closed-loop control, respectively. It is seen that the actuators effectively damp out the plate vibrations with the use of the closed-loop control. The dynamic responses of the delaminated smart composite plate are also presented in Figs. 3c and 3d for cases with and without feedback control, respectively. The same plate geometry and initial conditions are used as in the undelaminated case. Multiple through-the-width delaminations are assumed to be located on the midplane at distances 0.01905, 0.03175, 0.04445, and 0.05715 m measured from the clamped edge. The length β (nondimensionalized with respect to plate length) of each delamination is assumed to be 0.05. A comparison of Figs. 3b and 3d indicates that the control authority is weakened due to the presence of delaminations. In other words, vibration is being damped out at a slower rate in the presence of delaminations.

The first two bending modes of vibrations are presented in Figs. 4a and 4b for both the undelaminated and the delaminated cases. In this study a single through-the-width delamination of length 0.05 is placed on the midplane starting at 0.03175 m from the clamped edge. For such a small delamination, it is observed that the classical mode shapes (Figs. 4a and 4b) remain almost unchanged. However, the longitudinal strains corresponding to these modes, as shown in Figs. 5a and 5b, indicate clear differences between the undelaminated and the delaminated cases. This indicates that strains are a more sensitive measure of delamination and can be used as an effective parameter in detecting small delaminations in composites. For multiple delaminations, however, the mode shapes are significantly influenced due to an overall loss of rigidity in the plate (Figs. 6a and 6b).

Figures 7a–7c present the variation of natural frequencies with respect to aspect ratio a/h . The first natural frequency is highly overestimated by the classical theory (Fig. 7a), especially for thick plates, whereas the first-order and the higher-order theories are in good agreement. Larger differences between the theories are observed in Figs. 7b and 7c for the second bending and the first torsional natural frequencies, respectively. Even the first-order theory overpredicts these frequencies. The natural frequencies from the higher-order theory are smaller, as expected, because the transverse shear deformation is better approximated in this theory. These results indicate that it is necessary to include an accurate description of the transverse shear stresses that are important in composites due

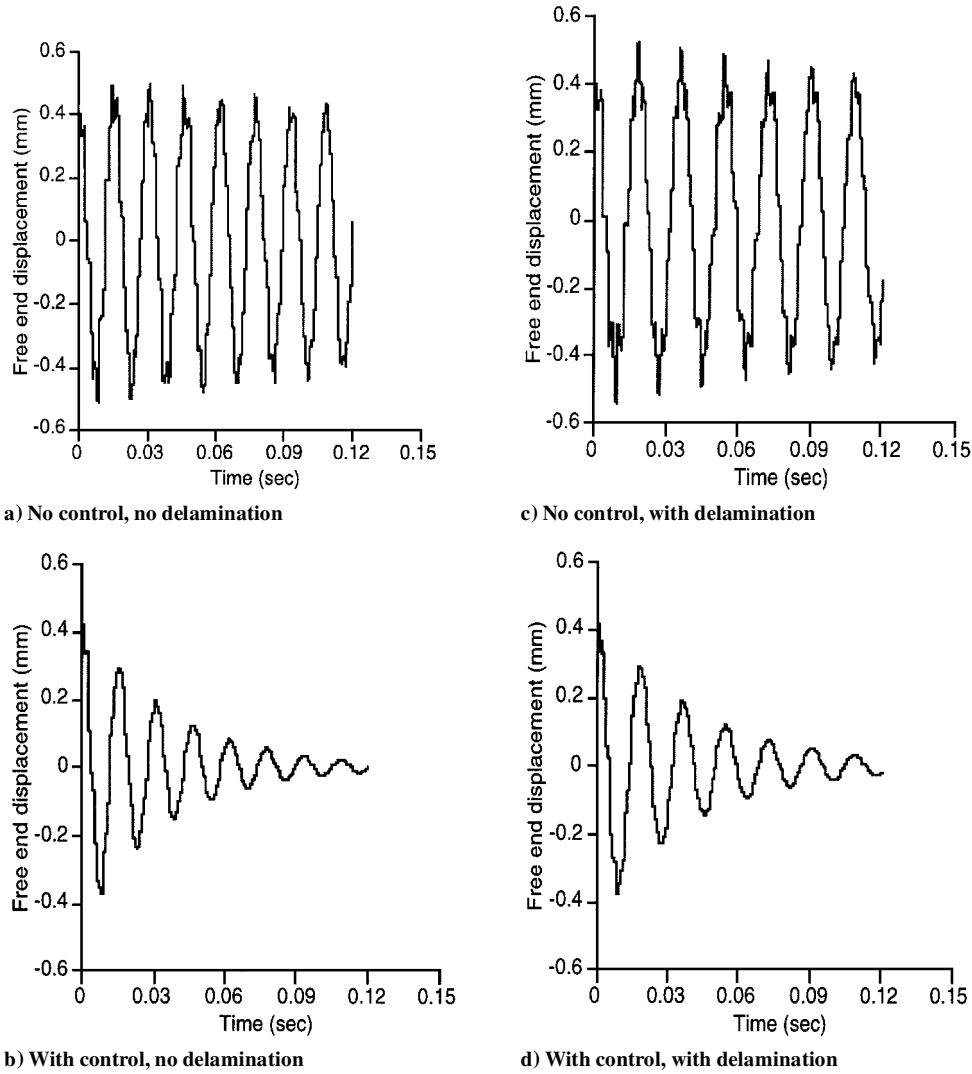


Fig. 3 Time history of free end displacement.

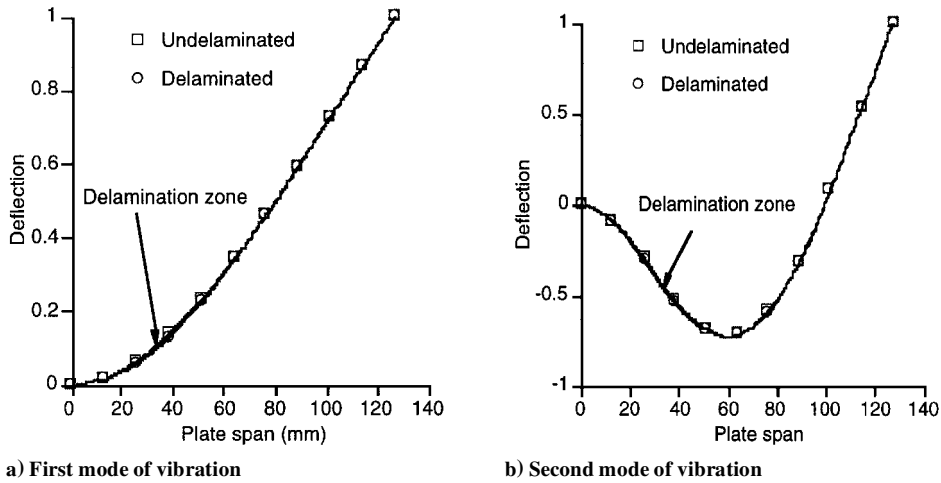


Fig. 4 Modes of vibration, with and without delamination.

to the large ratio between Young's moduli and the shear moduli. The transverse shear effects increase with plate thickness, resulting in larger deviations between the theories as a/h reduces.

Finally, the results of the present theory are compared with those obtained using classical laminate theory and the first-order theory for a delaminated plate with aspect ratio $a/h = 15.7$. It is assumed that a single through-the-width delamination of variable length β is located at midplane and is placed symmetrically with respect to

plate length. Figures 8a–8c present the variations of some natural frequencies of the plate with changes in the delamination length β . Again, for the first natural frequency, the first-order theory slightly overestimates the value, whereas the classical theory shows a significant deviation (Fig. 8a). The differences are more evident in higher natural frequencies (Figs. 7b and 7c). The higher-order theory once again yields the smallest values because of a more accurate representation of the transverse shear deformation. It is seen that the

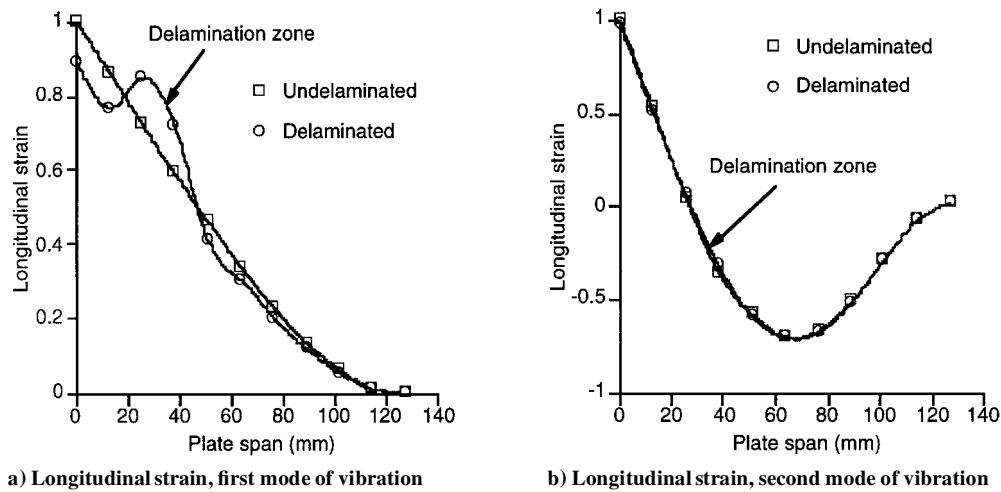


Fig. 5 Longitudinal strain distribution for the first two modes of vibration.

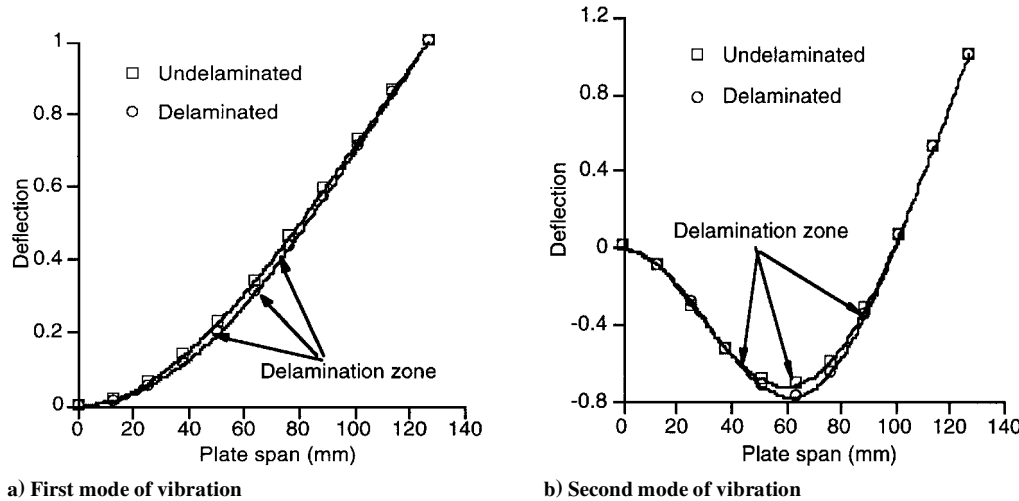


Fig. 6 Modes of vibration, multiple delaminations.

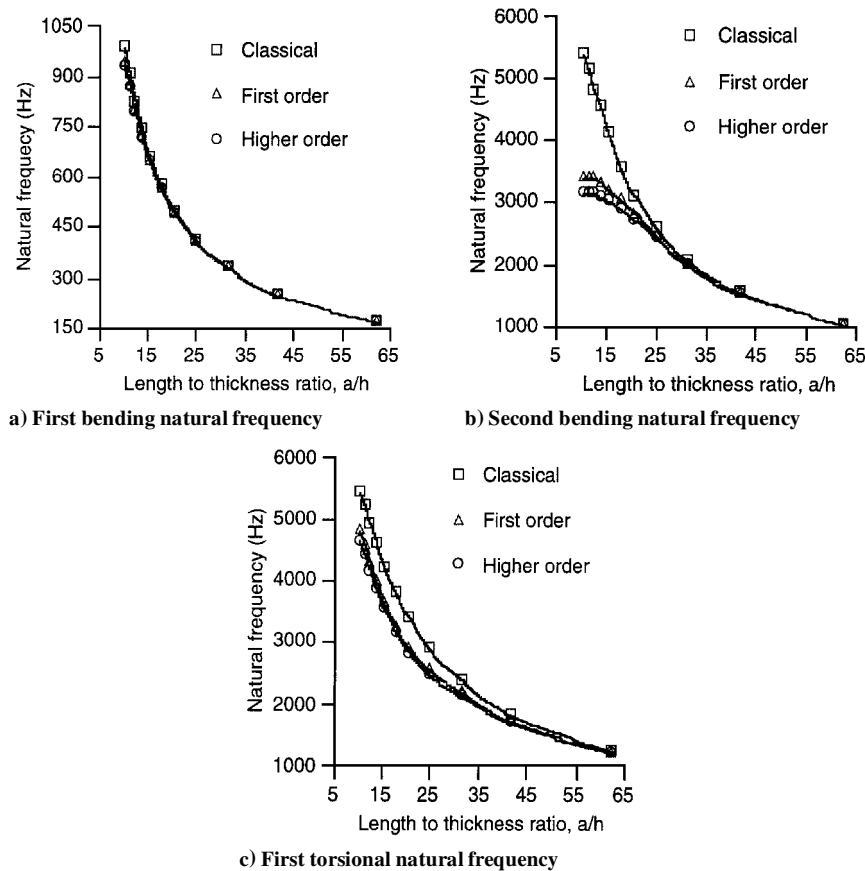


Fig. 7 Variation of natural frequencies with length-to-thickness ratio.

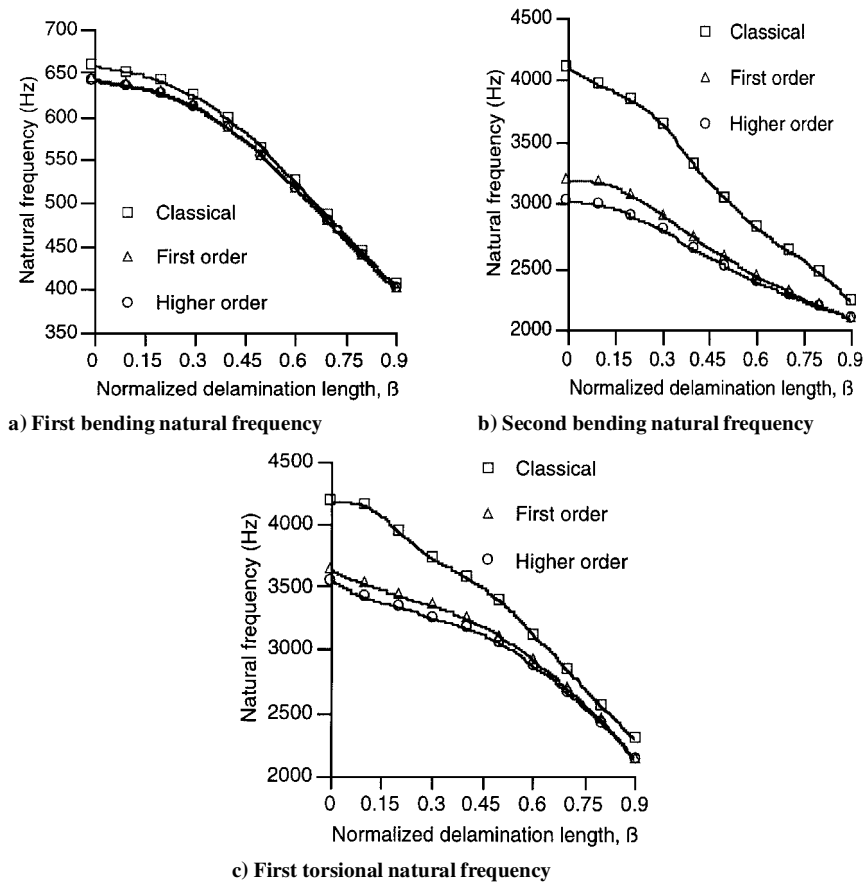


Fig. 8 Variation of natural frequencies with delamination length.

transverse shear effect becomes larger as the delamination length reduces. This can be explained as follows. For a short delamination length, the global dynamics of the plate are determined mainly by the total laminate thickness. Therefore, transverse shear effects are dominant in these cases. For relatively longer lengths, the dynamics of each thinner sublaminates become prevalent, thereby reducing the transverse effect.

Concluding Remarks

A general framework has been developed for the analysis of smart composite plates with surface bonded piezoelectric actuators and sensors in the presence of multiple delaminations. We have used a refined third-order theory that accurately captures the transverse shear deformation through the thickness of the smart composite laminate while satisfying the stress-free boundary conditions on the free surfaces, including the delaminated regions. The presence of preexisting single and multiple delaminations in the composite laminate at the layer interface has been studied. The following important observations have been made from this study:

- 1) The developed theory correlates well with experimental results.
- 2) Delaminations weaken the primary structure and reduce the closed-loop control authority.
- 3) Insignificant changes are observed in classical mode shapes when the delamination size is very small.
- 4) Significant changes are observed in the longitudinal strain distribution due to delamination. This indicates that strain can be a more effective measure in the detection of a small delamination in a composite structure.
- 5) For an undelaminated plate the natural frequencies are over-predicted by both the classical and the first-order theories compared with the higher-order theory. The deviations increase with plate thickness.
- 6) In the presence of delamination the natural frequencies are overestimated by both the classical and the first-order theories compared with the higher-order theory, particularly for higher frequencies. The deviations between the theories increase as the delamination length decreases. This indicates the importance of accurately

modeling the transverse shear stresses that are included in the higher-order theory.

Acknowledgments

The research was supported by the U.S. Air Force Office of Scientific Research, Grant F49620-96-0195, and the Technical Monitor was Brian Sanders.

References

- ¹Chattopadhyay, A., and Seeley, C. E., "A Higher Order Theory for Modeling Composite Laminates with Induced Strain Actuators," *Composites*, Vol. 28, Pt. B, 1997, pp. 243–252.
- ²Crawley, E. F., and Anderson, E. H., "Detailed Models of Piezoelectric Actuation of Beams," *Proceedings of the AIAA/ASME/ASCE/AHS/ASC 30th Structures, Structural Dynamics, and Materials Conference* (Mobile, AL), AIAA, Washington, DC, 1989, pp. 2000–2010.
- ³Chandrashekhara, K., and Agarwal, A. N., "Active Vibration Control of Laminated Composite Plates Using Piezoelectric Devices: A Finite Element Approach," *Journal of Intelligent Material Systems and Structures*, Vol. 4, Oct. 1993, pp. 496–508.
- ⁴Robbins, D. H., and Reddy, J. N., "Analysis of Piezoelectrically Actuated Beams Using a Layerwise Displacement Theory," *Computers and Structures*, Vol. 41, No. 2, 1991, pp. 265–279.
- ⁵Mitchell, J. A., and Reddy, J. N., "A Refined Hybrid Plate Theory for Composite Laminates with Piezoelectric Laminates," *International Journal of Solids and Structures*, Vol. 32, No. 16, 1995, pp. 2345–2367.
- ⁶Chattopadhyay, A., and Gu, H., "A New Higher-Order Plate Theory in Modeling Delamination Buckling of Composite Laminates," *AIAA Journal*, Vol. 32, No. 8, 1994, pp. 1709–1718.
- ⁷Seeley, C. E., and Chattopadhyay, A., "Modeling Delaminations in Smart Composite Laminates," *Proceedings of the AIAA/ASME/ASCE/AHS/ASC 37th Structures, Structural Dynamics, and Materials Conference and Adaptive Structures Forum* (Salt Lake City, UT), AIAA, Reston, VA, 1996, pp. 109–119.
- ⁸Yang, H. T. Y., and He, C. C., "Three-Dimensional Finite Element Analysis of Free Edge Stresses and Delamination of Composite Laminates," *Journal of Composite Materials*, Vol. 28, No. 15, 1994, pp. 1394–1412.
- ⁹Pavier, M. J., and Clarke, M. P., "A Specialized Composite Plate Element for Problems of Delamination Buckling and Growth," *Composite Structures*, Vol. 35, 1996, pp. 45–53.

¹⁰Barbero, E. J., and Reddy, J. N., "Modeling of Delamination in Composite Laminates Using a Layer-Wise Plate Theory," *International Journal of Solids and Structures*, Vol. 28, No. 3, 1991, pp. 373–388.

¹¹Chattopadhyay, A., and Gu, H., "Elasticity Approach for Delamination Buckling of Composite Beam Plates," *AIAA Journal*, Vol. 36, No. 8, 1998, pp. 1529–1534.

¹²Chattopadhyay, A., and Gu, H., "An Experimental Investigation of Delamination Buckling and Postbuckling of Composite Laminates," *Composites Science and Technology* (to be published).

¹³Keilers, C. H., and Chang, F. K., "Identifying Delamination in Composite Beams Using Built-In Piezoelectric: Part I—Experiments and Analysis, Part II—An identification Method," *Journal of Intelligent Material System and Structures*, Vol. 5, No. 5, 1995, pp. 649–663.

¹⁴Seeley, C. E., and Chattopadhyay, A., "Modeling of Adaptive Composites Including Debonding," *International Journal of Solids and Structures*

(to be published).

¹⁵Crawley, E. F., and Lazarus, K. B., "Induced Strain Actuation of Isotropic and Anisotropic Plates," *Proceedings of the AIAA/ASME/ASCE/AHS/ASC 30th Structures, Structural Dynamics, and Materials Conference* (Mobile, AL), AIAA, Washington, DC, 1989, pp. 2000–2010.

¹⁶Chattopadhyay, A., Dragomir-Daescu, D., and Gu, H., "Dynamic Response of Smart Composites with Delamination," *Proceedings of the International Workshop on Structural Health Monitoring*, Stanford Univ., Stanford, CA, 1997, pp. 729–740.

¹⁷Shen, M. H., and Grady, J. E., "Free Vibration of Delaminated Beams," NASA TM-105582, 1992.

G. M. Faeth
Editor-in-Chief